Spectroscopic evidence for photo-ionization wakes in Vela X-1 and 4U 1700-37

Kaper, L.; Hammerschlag - Hensberge, G.C.M.J.; Zuiderwijk, E.J.

Publication date
1994

Published in
Astronomy & Astrophysics

Astron. Astrophys. 289, 846–854 (1994)

ASTRONOMY AND ASTROPHYSICS

Spectroscopic evidence for photo-ionization wakes in Vela X-1 and 4U 1700−37*

L. Kaper[1,2], G. Hammerschlag-Hensberge[1], and E.J. Zuiderwijk[3,4]

[1] Astronomical Institute "Anton Pannekoek", University of Amsterdam, Kruislaan 403, NL-1098 SJ Amsterdam, The Netherlands
[2] Center for High Energy Astrophysics (CHEAF), Kruislaan 403, NL-1098 SJ Amsterdam, The Netherlands
[3] Kapteyn Astronomical Institute, Postbus 800, NL-9700 AV Groningen, The Netherlands
[4] Royal Greenwich Observatory, Madingley Road, Cambridge CB2 0EZ, England

Received 22 December 1993 / Accepted 12 April 1994

Abstract. We present high-resolution, high signal-to-noise spectra of HD77581 and HD153919, the optical counterparts of the high-mass X-ray binaries Vela X-1 and 4U 1700−37, respectively. The spectral lines exhibit variations related to the presence of the X-ray source in unprecedented detail. For HD77581, at inferior conjunction of the neutron star ($\phi = 0.5$), an extra absorption component appears in the blue wing of the absorption lines. This feature first increases in strength (up till binary phase $\phi = 0.6$) whereafter it slowly fades; at the same time it shifts towards higher negative velocities. The observed velocities are *low*: from -50 km s^{-1} at $\phi = 0.5$ up to -250 km s^{-1} at $\phi = 0.8$. For HD153919, the observed variations are similar in character, but stronger and more complicated. For both systems we find significant variations in the emission part of the P Cygni-type profiles.

Based on the phase dependence of the velocity and strength of the absorption component, we show that it is unlikely that this component is related to an accretion wake, or to a gas stream through the inner Lagrangean point. These structures, although most likely present in the system, are not capable of providing sufficient obscuration of the supergiant, that would give the observed absorption. We suggest that this absorption component results from the presence of a *photo-ionization wake* in the system that trails the X-ray source. Furthermore, we predict that variations in X-ray luminosity will induce changes in the geometrical structure of the photo-ionization wake which might explain the observed orbit-to-orbit variations.

Key words: stars: binaries: close – stars: early-type – stars: individual: HD77581 (Vela X-1) – stars: individual: HD153919 (4U 1700−37) – stars: mass loss – X-rays: stars

* Based on observations obtained with the CAT/CES combination at ESO, La Silla, Chile

1. Introduction

The stellar wind of an OB supergiant, which provides the mass flux to power the compact X-ray source in high-mass X-ray binaries (HMXBs) such as Vela X-1 and 4U 1700−37, is driven by radiation pressure exerted on wind plasma by scattering and absorption of photons in numerous spectral lines formed in the stellar wind. As a consequence of the statistical equilibrium, the spectral lines are concentrated around the maximum of the spectral energy distribution of the OB supergiant, i.e. in the extreme ultraviolet wavelength region. The acceleration mechanism of the wind can be influenced by the X-rays originating from the compact object, since these will enhance the degree of ionization in the surrounding wind region. Inside this Strömgren zone the radiative acceleration is quenched, because for this highly ionized plasma most spectral lines are at X-ray wavelengths, and cannot support the acceleration of the flow (MacGregor & Vitello 1982). Collisions between the (undisturbed) radiation-driven wind and the stagnant, highly ionized plasma inside the Strömgren zone will result in strong shocks and create dense sheets of gas trailing the X-ray source (Fransson & Fabian 1980). Because such a shock arises from the interaction between plasmas of different ionization state, this shock is referred to as a *photo-ionization wake*. Also other structures in the stellar wind are expected because of the presence of a compact object: an accretion wake that trails the compact object in its orbit, and which results from the highly supersonic orbital velocity ($\sim$ 50 Mach); a gas stream that leaves the primary at the side of the compact object and that is formed by tidal interaction between the two binary components.

Two-dimensional hydrodynamics calculations by Blondin & co-workers (1990, 1991), in which many effects influencing the wind dynamics around the compact object (gravitation, radiative acceleration, photo-ionization, X-ray heating/cooling etc.) are included, predict the shape and evolution of the above mentioned structures in wind-fed HMXBs. An important result is that for high X-ray luminosities the photo-ionization wake at the trailing border of the Strömgren zone dominates the accre-

tion flow. The geometrical extent of the photo-ionization wake depends on the size of the Strömgren zone.

Observational evidence for X-ray photo-ionization of wind material in HMXBs has been inferred from orbital variations in strong P Cygni lines present in their UV spectra (e.g. Dupree et al. 1980; Hammerschlag-Hensberge 1980), an effect predicted by Hatchett & McCray (1977). When the X-ray source moves in front of the supergiant (at orbital phase $\phi = 0.5$), the amount of blue-shifted P Cygni absorption diminishes, indicative of a Strömgren zone around the compact star.

Support from observations for the presence of dense slabs of material in the accretion flow in HMXBs can be found by monitoring these systems in different wavelength bands. X-ray observations show an increase in X-ray hardness ratio towards late orbital phases, i.e. when the X-ray source is nearing eclipse by the supergiant (Mason et al. 1976; Haberl et al. 1989; Haberl & White 1990). The emitted soft X-rays are thought to be (partly) absorbed by regions of higher density in the line of sight towards the X-ray source at late orbital phases. The change in strength of Raman-scattered emission lines in UV spectra of HD153919 with binary phase is consistent with these X-ray observations (Kaper et al. 1990). Because of the very small dimensions of the X-ray source, the X-ray observations enable inspection of a tiny column of material in the stellar wind. This means that changes in the X-ray hardness ratio with orbital phase can be caused by relatively small structures (such as an accretion wake) that obscure the X-ray source.

Optical spectra of bright HMXBs reveal enhancements in blue-shifted absorption in strong spectral lines during and after the passage of the compact object through the line of sight towards the supergiant. Because the optical light is predominantly emitted by the supergiant, any observed change in absorption strength of optical lines results from a variation in the number of absorbers integrated over a relatively large column of wind material (compared to the column in front of the X-ray source). Wallerstein (1974), Zuiderwijk et al. (1974), and Bessell et al. (1975) published Hα spectra of HD77581 showing periodic changes in this blue-shifted absorption. Zuiderwijk (1979, see also Sect. 3.1) reported that an extra absorption component is present in his Hβ data, variable both in strength and velocity. Zuiderwijk remarked that the behaviour of the Hβ line of HD77581 is remarkably similar to that of the Hα profile. For HD153919, Conti & Cowley (1975) mentioned that most absorption and emission lines show little, if any, variation with orbital phase. Like Fahlman & Walker (1980) they find that phase-dependent absorption components are present in the Hα and He I 5876 Å lines. Usually, this late-phase absorption is attributed to the presence of a gas stream in the system that partly obscures the supergiant. The nature of this stream is, however, not clear and widely different suggestions about its geometry have been put forward.

We should point out that radiation-driven winds also exhibit *intrinsic* variability (Prinja & Howarth 1986; Kaper 1993). In UV P Cygni lines, formed in the wind of (single) OB stars, discrete absorption components accelerate through the profiles on a timescale of days; discrete absorption components have, however, not been encountered in (the small number of) UV spectra of HMXBs. This kind of variability seems to be a fundamental property of radiation-driven winds (Howarth & Prinja 1989). Although the instability of the line-acceleration mechanism has been proposed to give rise to the occurrence of these absorption features (cf. Puls et al. 1993), detailed monitoring of these variations, resulting in e.g. the observed dependence on the stellar rotation period (Henrichs et al. 1988; Prinja 1988), shows that the origin of the variations is not yet fully understood (Kaper 1993). Strong optical lines of OB stars also show intrinsic variations of the stellar wind (e.g. Ebbets 1982; Fullerton et al. 1992). The observed acceleration of narrow absorption features towards higher negative velocities is similar to that observed in UV resonance lines. Simultaneous observations of strong optical and UV wind lines (cf. Kaper et al. 1994) suggest that these different lines reflect the same phenomenon.

To study the structure of the mass-accretion flow in HMXBs in detail, we observed two bright optical counterparts: HD77581 (Vela X-1) and HD153919 (4U 1700−37), taking advantage of the strong development in observing techniques over the last decade. For details about the observational history and the stellar parameters of HD77581 (Vela X-1) and HD153919 (4U 1700−37) we refer to Nagase (1989) and Heap & Corcoran (1992), respectively. Vela X-1 is an X-ray pulsar with a pulse period of $\sim$ 283 seconds (McClintock et al. 1976); for 4U 1700−37 no X-ray pulsations are found. For both systems the X-ray lightcurve exhibits a long eclipse in accordance with the probably large inclination of the orbital plane ($i \approx 90°$). The radial velocity curve of the supergiant in both systems is known; cf. Van Kerkwijk et al. (1994) for HD77581 and Hammerschlag-Hensberge (1978) for HD153919. In the next section we describe the reduction of the spectra we obtained. The results are presented in Sect. 3. We discuss in Sect. 4 how our results constrain on the geometry of the mass-accretion flow in these two HMXBs. In the last section we summarize our conclusions.

Table 1. Log of observations HD77581: 2-11 June 1992. All observations are 30 minutes exposures. Ephemeris*: Phase zero ≡ JD2444279.0466 ± 0.0037; P = 8.964416±0.000049 days (Deeter et al. 1987)

HD 77581			
He I 4471Å		Hβ	
JD-2448000 (mid-exp.)	orbital phase*	JD-2448000 (mid-exp.)	orbital phase*
776.522	.703	776.451	.695
776.544	.706	776.467	.697
777.488	.811	776.497	.700
777.544	.817	777.459	.808
782.535	.374	777.513	.814
783.484	.480	782.512	.371
783.537	.486	783.460	.477
784.476	.590	783.513	.483
784.533	.597	784.453	.588
		784.508	.594

Table 2. Log of observations HD153919: 2-11 June 1992. All observations are 30 minutes exposures. MJD = JD-2448000 and gives the mid-exposure time. Ephemeris*: Phase zero ≡ JD2446161.3400 ± 0.0030; P = 3.411652±0.000026 days (Haberl et al. 1989)

HD 153919					
He I 4471 Å		Hβ		He II 4686 Å	
MJD	orbital phase*	MJD	orbital phase*	MJD	orbital phase*
776.574	.560	776.683	.592	776.608	.570
776.785	.621	776.705	.598	776.651	.582
777.576	.853	776.755	.612	776.883	.650
777.710	.892	776.906	.657	777.602	.861
782.560	.314	777.631	.869	777.749	.904
782.761	.373	777.686	.885	777.797	.918
782.880	.408	777.840	.930	782 592	.323
783.612	.622	777.886	.944	782.794	.383
783.705	.650	782.636	.336	783.640	.631
783.790	.675	782.681	.349	783.737	.659
783.881	.701	782.828	.393	783.822	.684
784.576	.905	783.681	.643	784.608	.914
784.674	.934	783.765	.667	784.698	.941
784.782	.965	783.851	.692	784.814	.975
784.874	.992	784.636	.923		
		784.737	.952		
		784.842	.983		

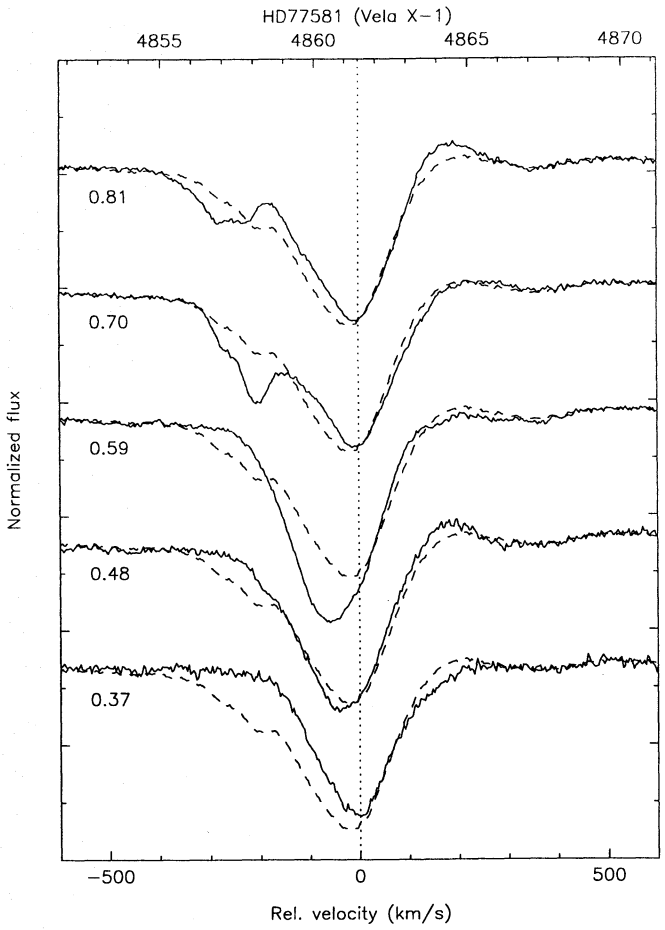

Fig. 1. Normalized Hβ profiles of HD77581 (Vela X-1). The spectra have been shifted vertically according to their orbital phase, indicated at the left side of each spectrum. The tickmarks on the vertical scale are placed at 10% intervals. The dashed line represents the average spectrum. Note, however, that the spectra at $\phi = 0.6$ and $\phi = 0.7$ are *not* sequential: we started the observations at $\phi = 0.7$

2. Observations

Spectra of HD77581 (B0.5 Iab, V = 6.9) and HD153919 (O6.5 Iaf$^+$, V = 6.5) were obtained with the Coudé Echelle Spectrograph (CES) attached to the Coudé Auxiliary Telescope at the European Southern Observatory in La Silla, Chile. In Table 1 and 2 we list the observing dates and corresponding orbital phases of the obtained spectra; the ephemeris used to calculate the orbital phase is from Deeter et al. (1987) and Haberl et al. (1989) for HD77581 and HD153919, respectively. We used the blue path and the short camera with a thinned, backside-illuminated CCD (RCA#9, 1024 × 640 pixels). Spectra were taken in the wavelength regions around He I 4471.48 Å, He II 4685.75 Å (the latter only for HD153919), and Hβ at 4861.33 Å. We monitored these lines during two shifts of three nights, from June 2nd to 5th and June 8th to 11th, 1992. In this way we covered almost two orbits of HD153919 (P_{orb} = 3.41 days) and part of an orbit of HD77581 (P_{orb} = 8.96 days).

With an exposure time of half an hour a signal-to-noise ratio of about 200 or more was obtained. Due to the high spectral resolution (R=60 000, i.e. ∼ 5 km s^{-1} per resolution element) and, consequently, the small spectral coverage of about 30 Å, we had to change the central wavelength frequently. To correct for any instrumental effects calibration frames (lamp flatfields and Th-Ar spectra) were obtained after each change of central wavelength.

The spectra were reduced using the MIDAS software package and an optimal extraction routine based on the method given by Horne (1986). The spectra were normalized using a second order polynomial fit to five carefully selected wavelength regions without spectral lines. The wavelength scale was converted to the system's rest-frame velocity scale, using $\gamma = -7$ and -64.5 km s^{-1} for HD77581 and HD153919, respectively (Van Paradijs et al. 1976; Gies 1987). We did not correct the spectra for the radial velocity of the star due to the orbital revolution. The K-amplitude of the radial-velocity curve of the supergiant is 20.8 km s^{-1} for HD77581 (Van Kerkwijk et al. 1994) and 19.0 km s^{-1} for HD153919 (Hammerschlag-Hensberge 1978).

3. Results

3.1. HD77581 (Vela X-1)

In Figs. 1 and 2 we show spectra of the Hβ profile and the He I line at 4471 Å for HD77581 as a function of binary phase. The displayed spectra are averages of two or three exposures taken

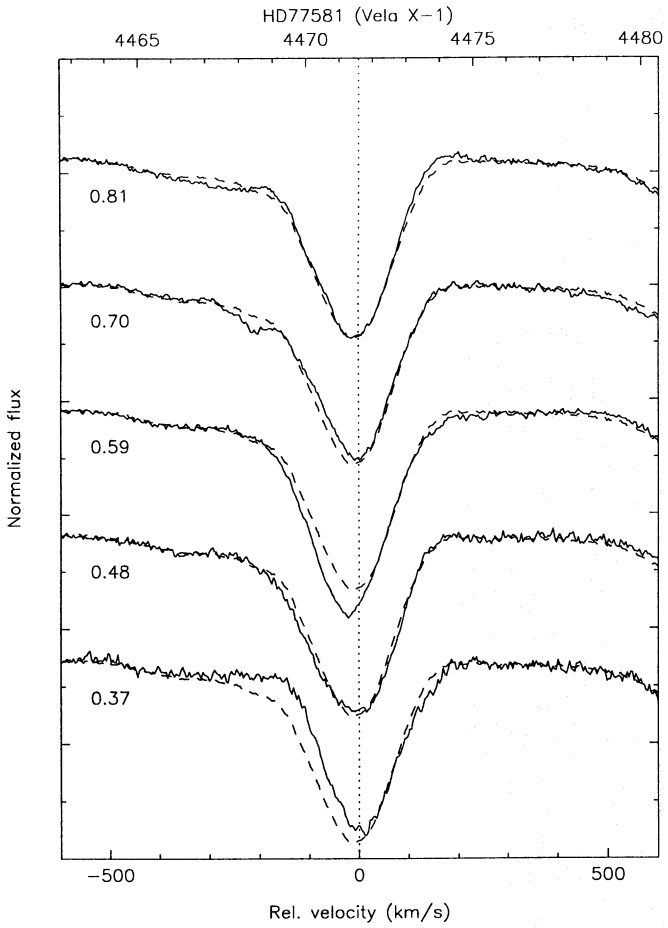

Fig. 2. As Fig. 1: the He I line of HD77581 at 4471 Å. The orbital variations as observed in the Hβ line also occur in this line, but are weaker

within one night, except for the spectra at $\phi = 0.37$ which are single. For comparison, the average of all exposures is indicated with a dashed line. On the vertical scale the tickmarks indicate steps of 0.1 measured in normalized flux (the continuum is normalized to one). We emphasize that we started the observations around $\phi = 0.7$, which means that the spectra at $\phi = 0.6$ and $\phi = 0.7$ are not sequential in time. Considering previous observations (see below) and the continuity of the variations in Figs. 1 and 2, we are convinced that the variations are induced by the binarity of the system and are not caused by intrinsic changes in the stellar wind.

In Fig. 1 one can clearly see an extra absorption component superposed on the photospheric absorption line (assumed to be symmetric) and starting at about -50 km s^{-1} around phase $\phi = 0.5$, when the X-ray source is in the line of sight. This extra component strengthens rapidly and reaches maximum strength at $\phi \sim 0.6$; subsequently, the absorption component shifts towards higher negative velocities and gets weaker. At $\phi = 0.8$ the component is still present, extending from ~ -175 to ~ -350 km s^{-1} and centered at -250 km s^{-1}. In the Hβ line, a significant red emission component is present in the spectra taken at $\phi = 0.5$ and $\phi = 0.8$.

These observations are similar to those presented by Zuiderwijk (1979) but of better quality because of the improved observing techniques. For comparison we reproduce in Fig. 3 phase-averaged Hβ profiles recorded on photographic (baked IIaO) emulsion during November 1975 and May 1976 with the (then) 1.5m ESO Coudé spectrograph. The photometric calibration of these spectra (at Hβ) leaves a lot to be desired (for details, see Zuiderwijk 1979), but the moving blue component is clearly visible. The velocities indicated were measured by means of a simple Gaussian fit to residual profiles obtained after subtraction of the (properly scaled) mean profile between phases 0.0 and 0.2, which is assumed to represent the "undisturbed" photospheric profile. Note that the spectra near phase 0.6 and 0.66 were taken 7 months apart. Taken together with the current data it is clear that, apart from moderate orbit-to-orbit variations, the phenomenon is stationary on longer timescales (> 700 orbital revolutions).

3.2. HD153919 (4U 1700−37)

The spectra of HD153919, displayed in Figs. 4, 5, and 6, clearly show the presence of orbital variations in its line profiles. The much better quality of the spectra compared to those of e.g. Conti & Cowley (1975) enabled a reliable detection of variability. The shown spectra are the averages of several individual exposures, some of them belonging to a different orbit (by which we neglect orbit-to-orbit variations, see next subsection). The Hβ line (Fig. 4) and the He I line at 4471 Å (Fig. 6) have P Cygni-type profiles and show a similar dependence on orbital phase. Around $\phi = 0.6$ the blue-shifted absorption strengthens greatly and widens, extending from ~ 50 to ~ -650 km s^{-1}. Around $\phi = 0.95$, when the X-ray source is almost in superior conjunction, the blue-shifted absorption is still stronger than at $\phi = 0.36$, and around -650 km s^{-1} a small absorption component is marginally visible, probably related to the extra absorption found at earlier phases. Also the emission component varies in strength. At $\phi \sim 0.6$ and especially at $\phi \sim 0.97$ the emission is stronger than at other phases.

The He II 4686 Å line is strongly in emission (Fig. 5). Most remarkable is the left wing of the profile, which shows a strange emission "shoulder" at $\phi = 0.35$ and which is very steep and linear around $\phi = 0.6$ (probably because of an enhancement of blue-shifted absorption). The variations in the He II line resemble somewhat the observed behaviour of this line in HDE226868/Cyg X-1 (Gies & Bolton 1986), although for HD153919 the line emission is much stronger. These authors explain the variations in the He II line of HDE226868 by focussing of the stellar wind in the direction of the compact object (cf. Friend & Castor 1982), that leads to a non-spherically symmetric density distribution of the stellar wind. If the supergiant approaches its critical Roche surface, the wind enhancement in the direction of the compact star will develop into a tidal stream (Blondin et al. 1991). Therefore, the variations observed in the He II line at 4686 Å of HD153919 (and HDE226868)

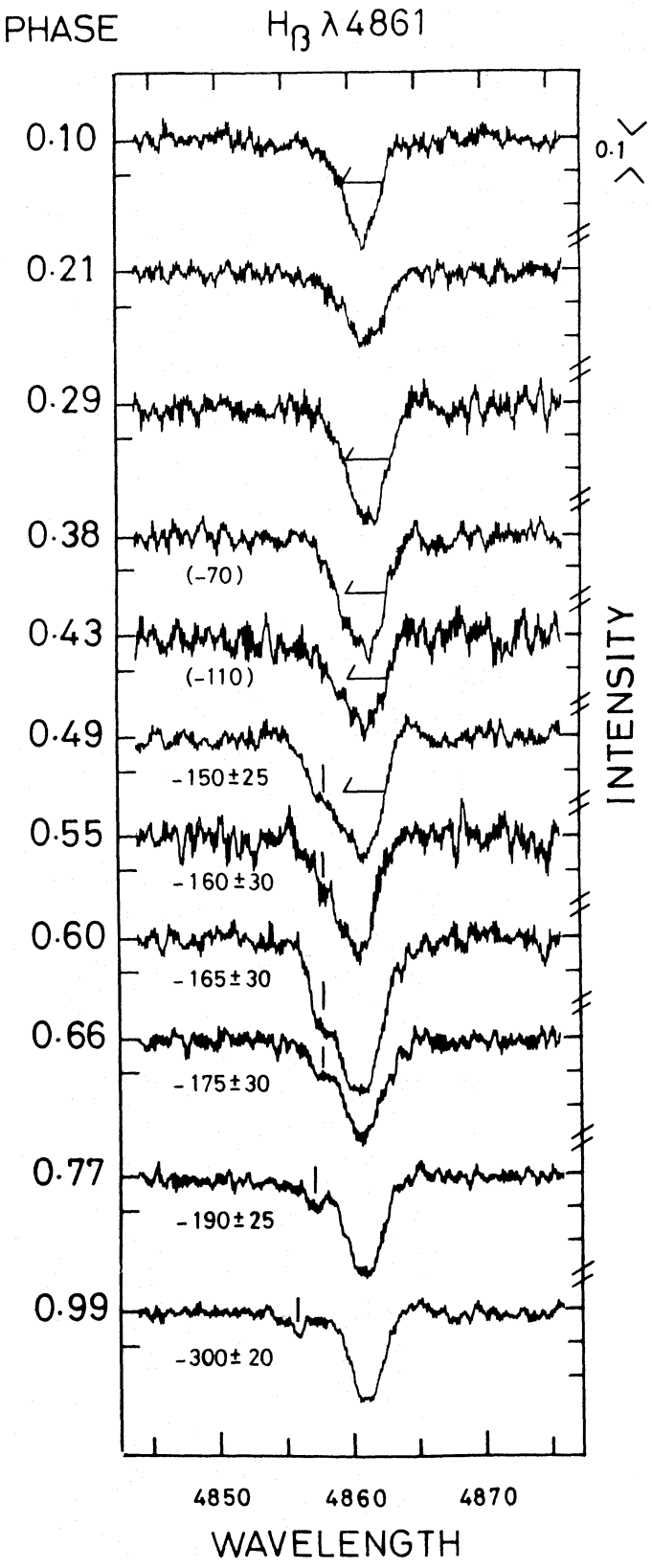

Fig. 3. Variations in the Hβ line of HD77581 as a function of orbital phase observed during 1975-1976; phase 0.0 corresponds to mid-X-ray eclipse. The width of the profile around phase zero is indicated in the other profiles up to phase 0.5. The apparent changes in strength of the steady component are most likely an artifact of photographic calibration uncertainties

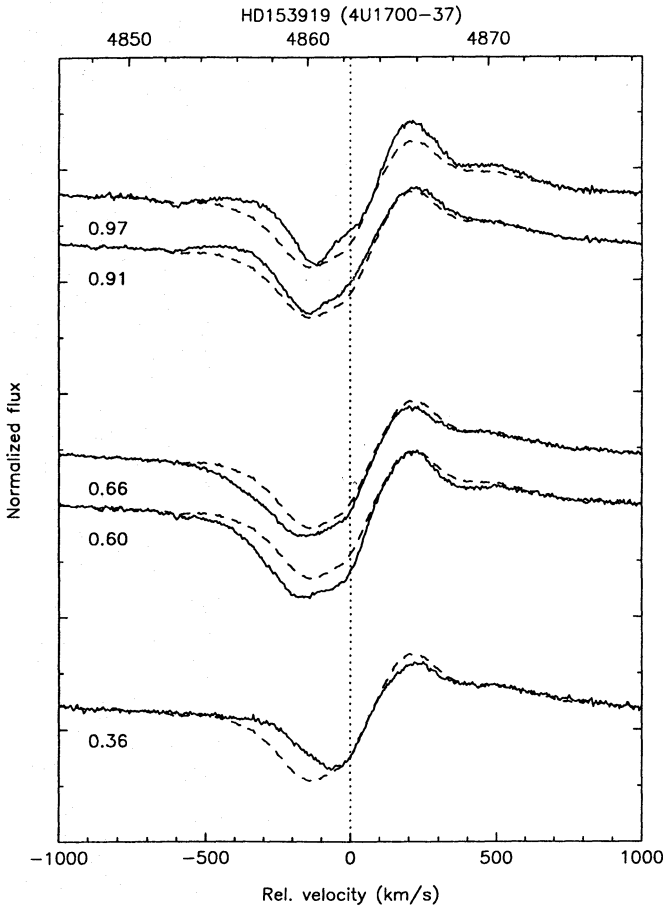

Fig. 4. As Fig. 1; The Hβ line of HD153919 is of P Cygni type and shows variations similar to those in the He I line (see Fig. 6). Shown are averages of several spectra, sometimes belonging to separate orbits, with respect to the average of all obtained spectra (dashed line). Note the strong increase in P Cygni emission at ϕ = 0.97; at this orbital phase some extra emission seems also present at the line center

could also be caused by the presence of a tidal stream in the system.

3.3. Orbit-to-orbit variations in HD153919

In Fig. 7 we compare spectra of HD153919 obtained in different orbits. From each orbit (we observed during two different orbits separated by about one orbit, see Sect. 2) two spectra are presented, taken around phase-point $\phi \sim 0.6$ when the extra, blue-shifted absorption is maximal. The spectra belonging to the same orbit are almost identical and can be recognized as such in the figure. In the top panel the He I line at 4471 Å is shown; for this line the found orbit-to-orbit variations are most pronounced. The deepest absorption (in comparison with the average ϕ = 0.35 spectrum, thick line) is reached in orbit 2. Although the spectra are independently normalized in the way described in Sect. 2, the large and systematic deviations (see also the Mg II line at 4481 Å) look like deviations one could encounter after a faulty normalization procedure. We have checked the normalization by fitting a spline through several points in the

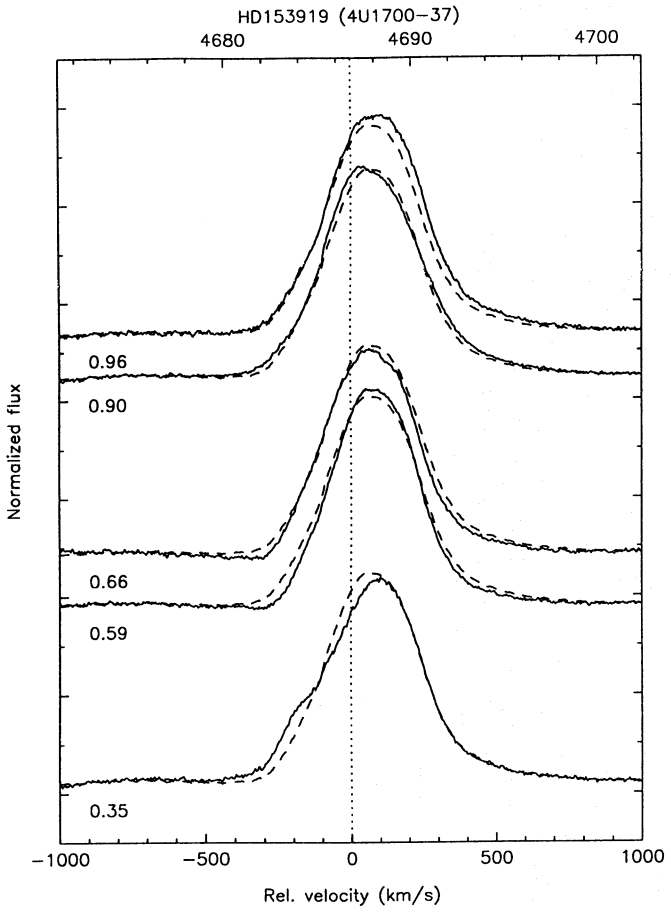

Fig. 5. As Fig. 1; The strong emission line of He II at 4686 Å, formed in the dense wind of HD153919, exhibits small but significant variations. The emission shoulder in the blue wing of the profile at ϕ = 0.35 is remarkable. The spectra around ϕ = 0.6 are consistent with extra blue-shifted absorption. The height of the emission peak is also variable

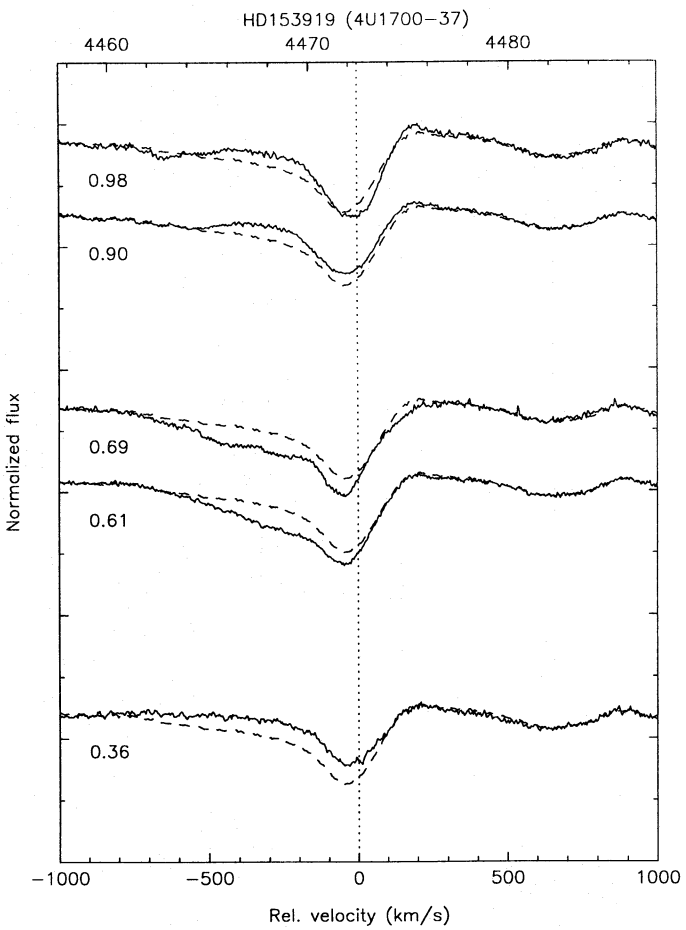

Fig. 6. As Fig. 1; The He I line of HD153919 at 4471 Å. Around ϕ = 0.6 the blue-shifted absorption gets much stronger over a wide velocity range, similar to the Hβ line displayed in Fig. 4

continuum, carefully selected by eye, and found similar results. The small wavelength region available makes a sound normalization, however, difficult. The He II line at 4686 Å (middle panel) and the Hβ line (bottom panel) also show small differences at similar phase-points in the two different orbits. The blue-shifted absorption in the Hβ line is deepest in orbit 1 (in contrast with the He I line). The normalization of the Hβ spectra is reliable. Although the relative behaviour with binary phase is similar, significant differences are found between lines from different orbits, but observed at approximately the same orbital phase.

4. Discussion

Many authors have suggested that the line-profile variability in optical spectra is due to an accretion wake or a tidal stream, similar to the interpretation of the observed X-ray absorption at late orbital phases, which is well explained by obscuration of the X-ray source by these structures (Blondin et al. 1990,1991). However, the relative velocity of the compact object with respect to the stellar wind causes the accretion wake to be directed away from the supergiant. A tidal stream through the inner Lagrangean point will be orientated along the line of centers (Blondin et al. 1991). In fact, Carlberg (1978) showed that no appreciable obscuration of the supergiant can be achieved by means of an accretion wake, given the expected characteristic dimension of about 10^{10} cm. It might be that close to ϕ = 0.5 the stellar disk is partly covered by the above mentioned structures, but this will probably result in only a very modest absorption enhancement in the spectral lines. That the amount of extra absorption observed at phases as late as ϕ = 0.8 is caused by an accretion wake and/or a tidal stream seems highly unlikely.

If one adopts a monotonic "beta"-velocity law for the stellar wind (with β = 0.8) and a terminal velocity v_∞ = 1105 km s^{-1} for HD77581 and v_∞ = 1820 km s^{-1} for HD153919 (Prinja et al. 1990), one finds for the wind velocities at the location of the compact star: v_w = 485 km s^{-1} and v_w = 1045 km s^{-1} for HD77581 and HD153919, respectively (using the orbital parameters of Nagase (1989) for Vela X-1, and of Heap & Corcoran (1992) for 4U 1700−37). These velocities are much higher than the typical velocities we find for the late-phase ab-

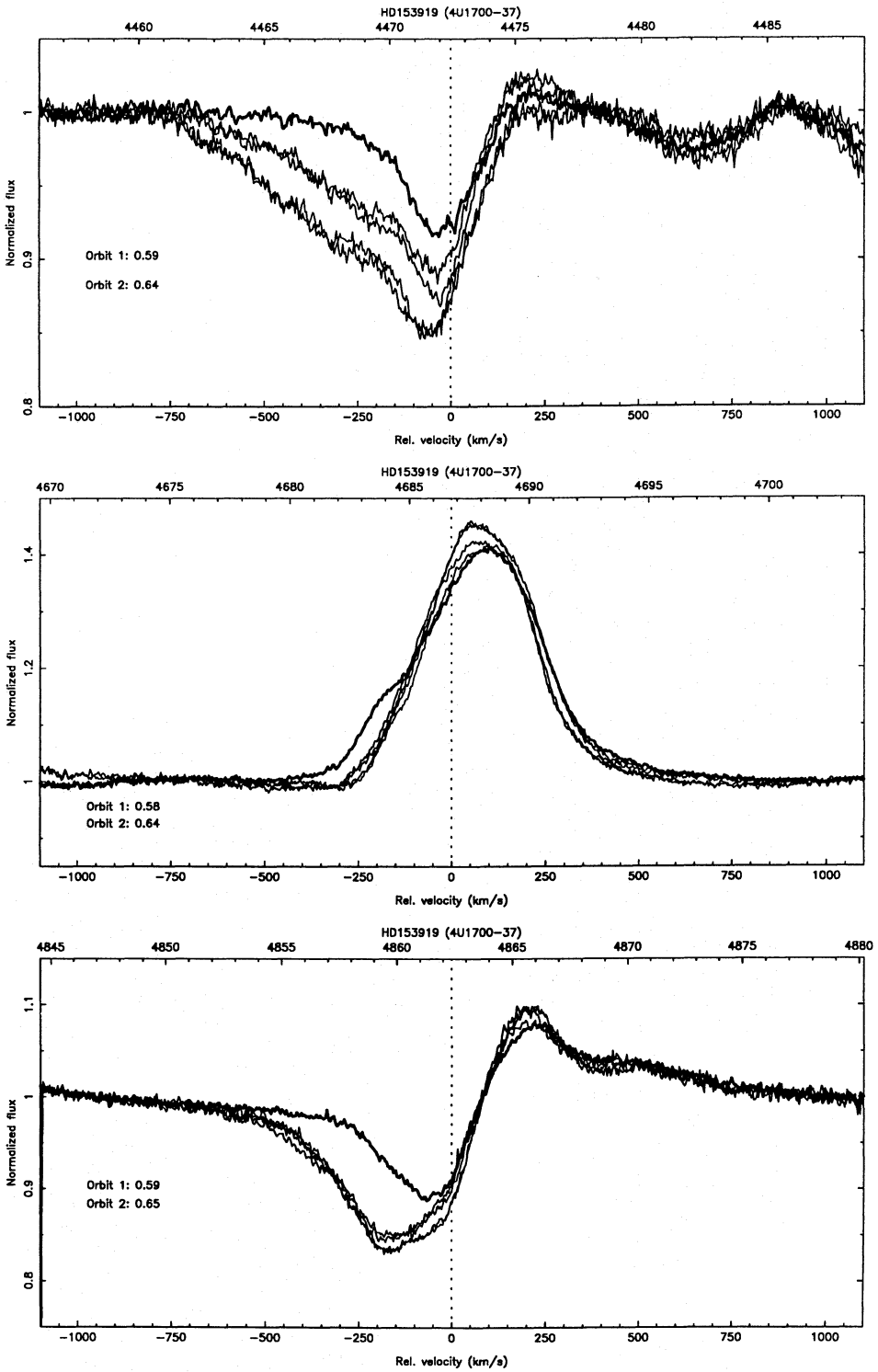

Fig. 7. The amplitude of the observed orbit-to-orbit variations in spectra of HD153919 is demonstrated for the three considered wavelength regions. In the top, middle, and bottom panel we show overplots of the He I line at 4471 Å, the He II line at 4686 Å, and the Hβ line at 4861 Å, respectively. A thick line represents the average $\phi = 0.35$ spectrum for comparison. The spectra belonging to the same orbit (the mean orbital phase indicated in the panel) are practically identical and can be recognized as such in the figure. The differences are most pronounced for the He I line

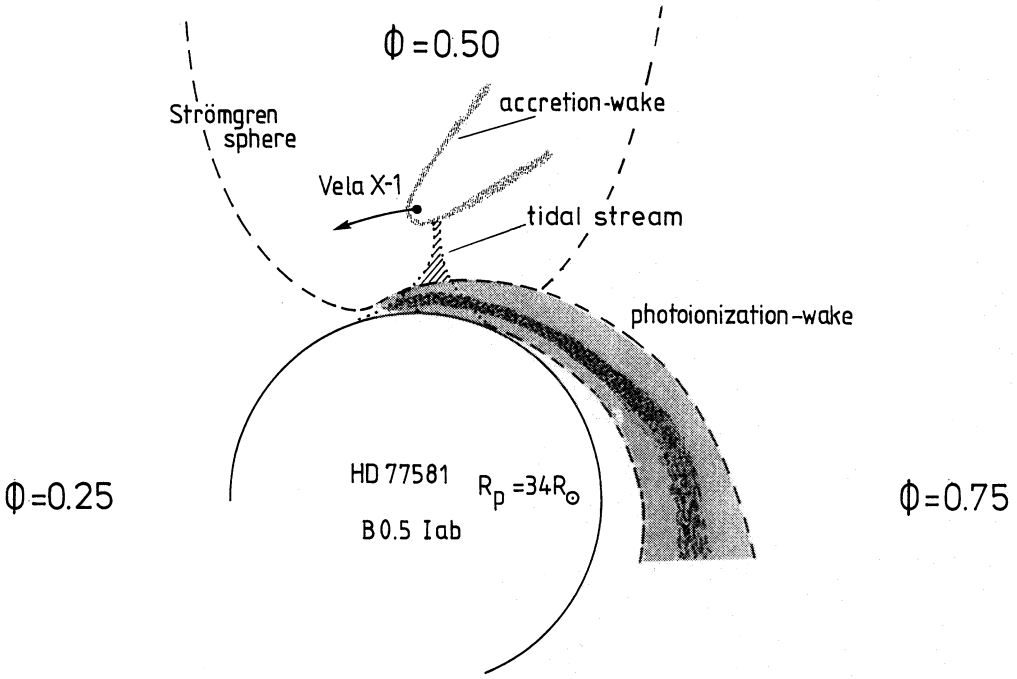

Fig. 8. A sketch of the different structures in the stellar wind of HD77581 based on observations at different orbital phases of the system. The position of the observer is shown for three orbital phases. X-ray observations indicate the presence of an accretion wake surrounding the compact object. A possible tidal stream is also illustrated in the figure. The position of the material giving rise to the extra absorption in the Hβ line of HD77581 is sketched by adopting v_∞ = 1100 km s^{-1} and a beta velocity law. We interpret the latter structure as a photo-ionization wake

sorption component. On the other hand, if the acceleration of the wind inside the Strömgren zone is negligible, the wind velocity at the position of the X-ray source is not much higher than at the border of the Strömgren zone. Inverting the problem, one can use the observed velocities to obtain an estimate of the (minimum) distance from the star at which the absorption takes place. In Fig. 8 we have sketched the expected position of the absorbing material in the wind of HD77581 based on this method. The sketched structure resembles the shape of a photo-ionization wake as calculated by Blondin et al. (1990, see e.g. their Fig. 15) very much. From Fig. 8 and the reasons given above, we propose that the observed velocity, strength, and phase-dependence of the extra blue-shifted absorption in optical spectra of HD77581 and HD153919 are in agreement with the properties of a photo-ionization wake.

The ionization parameter ξ (i.e. the ratio of X-ray flux and particle density, Tarter et al. 1969; Tarter & Salpeter 1969) is a measure for the ionization state of the plasma. Surfaces of constant ξ can be calculated and are in a good approximation congruent to surfaces of constant q, where q is a non-dimensional parameter defined by (Hatchett & McCray 1977):

$$q = \xi \frac{n_x D^2}{L_X} \quad (1)$$

The particle density at the location of the X-ray source is given by n_X, D is the orbital separation between the center of the supergiant and the X-ray source, and L_X is the X-ray luminosity. The size and shape of the Strömgren zone is thus determined by a certain value of q; surfaces of constant ξ close to the X-ray source are spheres and are labeled by high values of q (the smaller the enclosed volume, the higher the value of q). For $q < 1$ the surfaces are not closed anymore and are round-nosed cones surrounding the supergiant primary. For HD77581, independent evidence for an extended Strömgren zone ($q \sim 2$) in the wind comes from the observed orbital modulation of UV resonance lines (Dupree et al. 1980). Recently, Kaper et al. (1993) reanalysed the UV spectra of HD77581 and discovered that ionization effects also occur at very low wind velocities (up to $v_w \sim -250$ km s^{-1}), implying an even lower value of q. For such low values of q the numerical calculations of Blondin et al. (1990) show that the column density of the photo-ionization wake, which is located at the trailing border of the Strömgren zone, can become very large. For very small values of q the photo-ionization wake wraps around the supergiant, and can increase the observed column density even at late phases, possibly all the way into eclipse.

Although a low value for q is expected for HD153919 (4U 1700−37) as well (Hatchett & McCray 1977), no orbital modulation is observed in the UV resonance lines of this system. This may indicate that velocity and density of the stellar wind depend *non-monotonically* on radius (Kaper et al. 1993). In this way the Strömgren zone, which is certainly present in the wind of HD153919, could be hidden from detection in the UV resonance lines, because sufficient scattering ions are left *outside* the Strömgren zone to keep these profiles saturated.

If the X-ray luminosity increases, the ionization parameter ξ becomes larger under the assumption that the density structure of the stellar wind remains fixed. We should add here that the X-ray luminosity itself depends on the density and velocity of the wind at the position of the X-ray source. In the case of larger ξ, the border of the Strömgren zone will coincide with a surface of lower q, and vice versa. As a photo-ionization wake will be close to or at the trailing border of the Strömgren zone, the geometry of the photo-ionization wake will depend on the shape of the Strömgren zone. For Vela X-1 and 4U 1700−37, the observed X-ray luminosity is highly variable (Watson & Griffiths 1977;

Haberl et al. 1989). Large flares, with sometimes a factor of 100 increase in X-ray luminosity, do occur on a time scale of a day. This will cause variations in ξ and therefore a changing size of the Strömgren zone. The precise phase and velocity dependence of the late-phase absorption, if caused by a photo-ionization wake, will thus be a function of the X-ray luminosity, which could cause the observed orbit-to-orbit variations.

5. Summary

Strong optical lines in spectra of HD77581 and HD153919 show an increase in blue-shifted absorption during and after the passage of the X-ray source through the line of sight towards the supergiant. We argue that both the accretion wake surrounding the compact object and a possible gas stream in the system caused by tidal forces cannot be the cause of the observed obscuration of the supergiant. The observed orbital modulation of UV resonance lines formed in the wind of HD77581 indicates that the Strömgren zone around the X-ray source is very extended. As a consequence of the acceleration mechanism of the wind, a dense photo-ionization wake at the trailing border of this Strömgren zone is expected. The large extent of the Strömgren zone will result in low velocity of the gas inside the photo-ionization wake (because it is close to the supergiant) and also sufficient coverage of the supergiant. Orbit-to-orbit variations could result from changes in geometry of the photo-ionization wake that result from variations in X-ray luminosity.

Acknowledgements. We thank M.H. van Kerkwijk and J.H. Telting for loan of reduction programmes and for helpful discussions. The referee M. Pakull is acknowledged for his critical comments that helped to improve the paper. We appreciate the support of the night assistants at ESO Garching and La Silla during the remote control observations. LK acknowledges support from the Netherlands Foundation for Research in Astronomy with financial aid from the Netherlands Organization for Scientific Research (NWO) under grant 782-371-037

References

Bessell M.S., Vidal N.V., Wickramasinghe D.T., 1975, ApJ 195, L117
Blondin J.M., Kallman T.R., Fryxell B.A., Taam R.E., 1990, ApJ 356, 591
Blondin J.M., Stevens I.R., Kallman T.R., 1991, ApJ 371, 684
Carlberg R.G., 1978, Ph.D. thesis, Univ. of British Columbia
Conti P.S., Cowley A.P., 1975, ApJ 200, 133
Deeter J., Boynton P., Shibazaki N. et al., 1987, AJ 93, 877
Dupree A.K., et al., 1980, ApJ 238, 969
Ebbets D., 1982, ApJS 48, 399
Fahlman G.G., Walker G.A.H., 1980, ApJ 240, 169
Fransson C., Fabian A.C., 1980, A&A 87, 102
Friend D.B., Castor J.I., 1982, ApJ 261, 293
Fullerton A.W., Gies D.R., Bolton C.T., 1992, ApJ 390, 650
Gies D.R., 1987, ApJS 64,545
Gies D.R., Bolton C.T., 1986, ApJ 304, 371
Haberl F., White N.E., 1990, ApJ 361, 225
Haberl F., White N.E., Kallman T.R., 1989, ApJ 343, 409
Hammerschlag-Hensberge G., 1978, A&A 64, 399
Hammerschlag-Hensberge G., 1980, in Proc. 2nd European IUE Conf., Eds. Battrick & Mort, ESA SP-157, p. lix
Hatchett S., McCray R., 1977, ApJ 211, 552
Heap S.R., Corcoran M.F., 1992, ApJ 387, 340
Henrichs H.F., Kaper L., Zwarthoed G.A.A., 1988, in Proc. "A Decade of UV Astronomy with the IUE Satellite", ESA SP-281, Vol. 2, p. 145
Horne K., 1986, PASP 98, 609
Howarth I.D., Prinja R.K., 1989, ApJS 69, 527
Kaper L., 1993, Ph.D. thesis, University of Amsterdam
Kaper L., Hammerschlag-Hensberge G., Takens R.J., 1990, Nat 347, 652
Kaper L., Hammerschlag-Hensberge G., van Loon J.Th., 1993, A&A 279, 485
Kaper L., Henrichs H.F., Ando H. et al. 1994, submitted to A&A
Mason K.O., Branduardi G., Sanford P.W., 1976, ApJ 203, L29
MacGregor K.B., Vitello P.A.J., 1982, ApJ 259, 267
McClintock J.E., Rappaport S., Joss P.C. et al., 1976, ApJ 206, L99
Nagase F., 1989, PASJ 41, 1
Prinja R.K., 1988, MNRAS 231, 21P
Prinja R.K., Howarth I.D., 1986, ApJS 61, 357
Prinja R.K., Barlow M.J., Howarth I.D., 1990, ApJ 361, 607
Puls J., Owocki S.P., Fullerton A.W., 1993, A&A 279, 457
Van Kerkwijk M.H., Van Paradijs J.A., Zuiderwijk E.J. et al., 1994, submitted to A&A
Tarter B.C., Salpeter E.E., 1969, ApJ 156, 953
Tarter B.C., Tucker W.H., Salpeter E.E., 1969, ApJ 156, 943
Van Paradijs J.A., Hammerschlag-Hensberge G., Van den Heuvel E.P.J. et al., 1976, Nat 259, 547
Wallerstein G., 1974, ApJ 194, 451
Watson M.G., Griffiths R.E., 1977, MNRAS 178, 513
Zuiderwijk E.J., 1979, Ph.D. thesis, University of Amsterdam
Zuiderwijk E.J., Van den Heuvel E.P.J., Hensberge G., 1974, A&A 35, 353

This article was processed by the author using Springer-Verlag LaTeX A&A style file version 3.